Journal Pre-proof

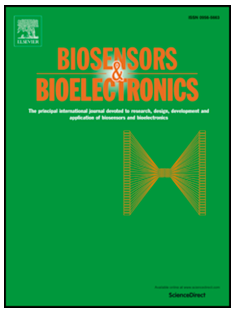

Designed antifouling peptides planted in conducting polymers through controlled partial doping for electrochemical detection of biomarkers in human serum

Rui Han, Guixiang Wang, Zhenying Xu, Leyao Zhang, Qun Li, Yinfeng Han, Xiliang Luo

PII: S0956-5663(20)30312-2

DOI: https://doi.org/10.1016/j.bios.2020.112317

Reference: BIOS 112317

To appear in: *Biosensors and Bioelectronics*

Received Date: 8 January 2020

Revised Date: 13 May 2020

Accepted Date: 19 May 2020

Please cite this article as: Han, R., Wang, G., Xu, Z., Zhang, L., Li, Q., Han, Y., Luo, X., Designed antifouling peptides planted in conducting polymers through controlled partial doping for electrochemical detection of biomarkers in human serum, *Biosensors and Bioelectronics* (2020), doi: https://doi.org/10.1016/j.bios.2020.112317.

CRediT author statement

Guixiang Wang: Conceptualization, Methodology, Writing- Original draft preparation. **Rui Han:** Data curation, Writing- Original draft preparation. **Zhenying Xu:** Data curation, Investigation. **Leyao Zhang:** Writing- Reviewing and Editing, Disscussion. **Qun Li:** Writing- Reviewing and Editing. **Yinfeng Han:** Writing- Reviewing and Editing. **Xiliang Luo:** Supervision, Visualization, Conceptualization, Writing- Reviewing and Editing.

Designed antifouling peptides planted in conducting polymers through controlled partial doping for electrochemical detection of biomarkers in human serum

Rui Han,[a] Guixiang Wang,[a,b,*] Zhenying Xu,[a] Leyao Zhang,[a] Qun Li,[b] Yinfeng Han,[b] Xiliang Luo[a,*]

[a] Key Laboratory of Optic-electric Sensing and Analytical Chemistry for Life Science, MOE, Shandong Key Laboratory of Biochemical Analysis, College of Chemistry and Molecular Engineering, Qingdao University of Science and Technology, Qingdao 266042, China.

[b] College of Chemistry and Chemical Engineering, Taishan University, Taian 271021, China.

* Corresponding author, E-mail: *wangguixiang@tsu.edu.cn*; xiliangluo@qust.edu.cn; Fax: +8653284022681; Tel: +86 53284022990

Abstract

An antifouling electrochemical biosensing platform was constructed based on conducting polymer poly(3,4-ethylenedioxythiophene) (PEDOT) planted with designed peptides. The designed peptides containing doping and antifouling sequences were anchored to an electrode surface, followed by the electrochemical polymerization of PEDOT. The negatively charged doping sequence of the peptide was gradually doped into the PEDOT during the polymerization process, and by controlling the polymerization time, it was able to exactly dope the whole doping sequence into the PEDOT film, leaving the antifouling sequence of the peptide stretched out of the PEDOT surface. Therefore, an excellent conducting and antifouling platform was constructed just like planting a peptide tree in the PEDOT soil. With antibodies immobilized on the peptide, an antifouling electrochemical biosensor for the detection of a typical biomarker CA15-3 was developed. Owing to the unique properties of the conducting polymer PEDOT and the antifouling peptide, the electrochemical biosensor exhibited high sensitivity and long-term stability, and it was capable of detecting CA15-3 in serum of breast cancer patients without suffering from biofouling. The strategy of planting designed antifouling peptides in conducting polymers offered an effective way to develop electrochemical sensors for practical biomarker assaying in complex biological samples.

Keywords: Functional peptide; Conducting polymer; PEDOT; Antifouling biosensor; CA15-3

1. Introduction

Direct, accurate and fast detection of disease biomarkers in complex biological media is of great significance for early clinical diagnosis (Vaisocherová et al. 2015; Wu and Qu 2015). Owing to their unique physical and chemical properties, conducting polymers have found broad applications in the development of sensing systems, and various electrochemical biosensors capable of detecting biomarkers have been constructed utilizing different conducting polymers (Liu et al. 2019a; Wang et al. 2018a; Wu et al. 2019). Although conducting polymer modified electrodes have exhibited considerable success in biosensing applications, enormous challenge still exists when performed in complex biological samples due to the nonspecific adsorption of various proteins on electrode surfaces, which leads to poor sensitivity and even causes electrode malfunction (Xia et al. 2019). To reduce nonspecific adsorption, an effective way is the construction of antifouling sensing interfaces, and different electrochemical antifouling biosensors based on conducting polymers have been developed.

Generally, there are three different strategies to fabricate conducting polymer based electrochemical biosensors with antifouling capabilities. The first strategy is copolymerization. Antifouling materials (such as polyethylene glycol (Cui et al. 2016), and hyaluronic acid (Wang et al. 2016)) doped conducting polymer poly(3,4-ethylenedioxythiophene) (PEDOT) are electrochemically polymerized on the electrode surface, and then bio-recognition elements (AFP antibody, CEA, and etc.)

are immobilized on the antifouling materials to construct the biosensor. The second strategy is to deposit conducting polymers (polyaniline (PANI) (Hui et al. 2017; Liu et al. 2018; Liu et al. 2019b) or PEDOT (Wang et al. 2017)) on the electrode surfaces, and then immobilize the antifouling materials and the bio-recognition molecules in turn (Hui et al. 2017; Wang et al. 2017) to fabricate biosensors. The third strategy is to synthesize antifouling functional conducting polymer monomers (such as sulfobetaine-EDOT (Cao et al. 2016; Wu et al. 2018), phosphocholine-EDOT (Liu et al. 2017) and hyperbranched polyglycerol-EDOT (Ma et al. 2019)), and then electrodeposit them on the electrode surfaces, to directly detect small molecules like glucose (Wu et al. 2018) or dopamine (Liu et al. 2017), or to prepare biosensors after immobilization of bio-recognition molecules such as AFP antibody (Ma et al. 2019). The first method is simple, but most of the antifouling materials are entrapped in the conducting polymers, and only those exposed on the surface can exhibit antifouling capability. The second method requires the conducting polymers to have anchoring functional groups, for conducting polymers that have no active functional groups, such as PEDOT, they need to be doped (Wang et al. 2017) or modified (Ma et al. 2019) with other materials to meet the requirements. What's more, the conductivity and stability of the conducting polymers will be affected after the immobilization of antifouling materials. For the third method, antifouling functional monomers are not currently commercialized, and the synthesis of such monomers is complex and time-consuming.

In this work, we have creatively designed a multifunctional peptide with

sequence of CAEAEPPPPQEQKQEQK combining the doping and antifouling functions for the first time, enabling one end of the peptide to be doped into conducting polymer PEDOT, and the other end of the peptide anchored on the PEDOT surface. The designed peptide can be self-assembled onto the surface of gold nanoparticles (AuNPs) electrodeposited on a glassy carbon electrode (GCE) through the gold-sulphur bond (thiol comes from cysteine (C) of the peptide). The AEAE sequence (doping part) connected to the cysteine of the peptide is negatively charged and can be used as dopant for PEDOT electropolymerization. We can precisely control the doping part to be exactly doped into the PEDOT to form a conducting thin film, which can remarkably enhance the conductivity and stability of the substrate, and allow the antifouling QEQKQEQK sequence (antifouling part) to be planted in the PEDOT film. The linker PPPP sequence between the doping and antifouling parts is beneficial for the QEQKQEQK to form α-helical confirmation, which facilitates the formation of well-packed antifouling layer (Nowinski et al. 2012). The antibody of CA15-3, an important prognosis and recurrence diagnosis indicator of breast cancer (Ge et al. 2017; Liu et al. 2011; Martín et al. 2015), was used as an example to be immobilized on the antifouling sequence of QEQKQEQK, and the constructed antifouling electrochemical biosensor was successfully applied to detect CA15-3 in the serum of breast cancer patients (As illustrated in Scheme 1).

2. Materials and methods

2.1. Reagents

Multifunctional peptide (CAEAEPPPPQEQKQEQK, purity > 95%) and the reference peptide (CPPPPQEQKQEQK, purity > 95%) were designed by the authors, and synthesized by the Bank peptide biological technology Co. Ltd. (Hefei, China) and purified by high-performance liquid chromatography (HPLC). Anti-CA15-3 (Ab), CA15-3 and CA12-5 were purchased from Abcam (Cambridge, UK). 4-ethylenedioxythiophene (EDOT), 1-ethyl-3-(3-dimethyl- aminopropyl) carbodiimide (EDC)) and N-hydroxysuccinimde (NHS) were obtained from Aladdin regent (Shanghai, China). Bovine serum albumin (BSA), human serum albumin (HSA), myoglobin (Mb), lysozyme (Lys), carcinoembryonic antigen (CEA), alpha fetoprotein (AFP) and prostatic specific antigen (PSA) were purchased from Adamas-beta reagent (Shanghai, China). Dulbecco's modified eagle's medium (DMEM) was purchased from Sigma (Aldrich, St. Louis, MO). Human serum samples of healthy people and breast cancer patients were provided by the Eighth People's Hospital of Qingdao (Qingdao, China), and the informed consent for use of the human serum was obtained. All the sample preparation was authorized by an institutional review board of the Eighth People's Hospital of Qingdao and was performed in compliance with the institutional guidelines and relevant laws. Other chemicals were of analytical purity or better and used as supplied. Millipore water with a resistivity greater than 18 MΩ from a Milli-Q water purifying system was used in all experiments. Unless otherwise stated, all peptides used in this paper are multifunctional peptides by default.

2.2. Apparatus

Electrochemical measurements and electrodepositions were performed with a CHI 660E electrochemical workstation (Shanghai Chenhua Apparatus Corporation, China) with a conventional three-electrode electrochemical system composed of glassy carbon electrode (GCE, working electrode), saturated calomel electrode (SCE, reference electrode) and platinum wire electrode (auxiliary electrode). All the electrochemical experiences were performed at indoor temperature. Differential pulse voltammetry (DPV) measurements with the potential range from −0.2 to 0.6 V at amplitude of 50 mV, potential increment of 4.0 mV and pulse period of 0.5 s, were performed in 5.0 mM $[Fe(CN)_6]^{3-/4-}$ phosphate buffer saline (PBS, 10 mM, pH 7.4) containing 0.1 M KCl. The parameters of Amperometric *i-t* curve used for electrodeposition were included constant potential of 1.0 V and different running time.

X-ray photoelectron spectroscopy (XPS) was performed to monitor element concentrations using ESCALAB 250Xi spectrometer (Thermo-VG Fisher Scientific, USA) with a monochromatic Al Kα X-ray source (15 kV), as well as all spectra were normalized by value of the C (1s) peak (284.6 eV). Circular dichroism (CD) of the peptide was characterized by a Jasco J-1100 Circular Dichroism Spectrophotometer (Jasco, Japan). The hydrophilia of electrode surfaces was characterized with the JC2000D1 Instrument (Zhongchen Instrument, China), and the Zeta potentials was measured with Nano-ZS Zetasizer ZEN3600 (Malvern, U.K.). The surface protein adsorption was supervised using TCS-SP5 confocal laser microscope (Leica,

Germany) and SPR instrument (BioNavis 200, Finland).

2.3. Characterization of the peptide

The relationship between net charge and pH of peptides was investigated, and charge information of peptides was judged by Zeta potential. The secondary structure information of the reference peptide was examined via CD spectra in the wavelength range of 190-300 nm with a step width of 0.2 nm. Water contact angle was measured using the sessile drop method to examine the hydrophilicity of the surface with or without peptide.

Then, a SPR Navi 200A instrument equipped with a 670 nm laser was used to measure the protein-nonspecific adsorption onto the Au chip surface with or without the reference peptide. Firstly, PBS (pH 7.4, 10 mM) was flowed over the surface at a flow rate of 50 mL min^{-1}, then the surface was exposed to 10 mg mL^{-1} BSA for 15 min at a flow rate of 25 mL min^{-1}, and next rinsed with PBS at a flow rate of 50 mL min^{-1} until no further change in the SPR angle (ΔSPR). The ΔSPR was recorded before and after the protein adsorption and was used to quantify the amount of protein adsorbed on the surface. It has been reported that the change for ΔSPR of 1° was calculated to correspond to a surface protein adsorbing capacity of 592.4 ng cm^{-2} (Ye et al. 2016).

2.4. Fabrication of electrochemical biosensor

The GCE was polished with 0.3 and 0.05 μm alumina slurry in turn to make it a

mirror-shaped surface followed by ultrasonic cleaning in anhydrous ethanol and Millipore water for 2 min, respectively. Afterward, AuNPs were electrodeposited at −1.5 V to 0.5 V onto the electrode by cyclic voltammetry in 0.5 mM chloroauric acid ($HAuCl_4$) solution including 0.5 M KNO_3 (AuNP/GCE). Multifunctional peptide was self-assembled onto AuNPs electrodeposited on GCE by soaking in 0.14 mM peptide aqueous solution and incubated for over 12 h at room temperature, followed by a thorough rinse with water (Pep/AuNP/GCE). And then, direct electrochemical polymerization of EDOT monomers was performed in 5 mL of aqueous solution containing 7.4 mM EDOT, which was evenly dispersed in water by ultrasonication before polymerization (PEDOT/Pep/AuNP/GCE). The carboxylic groups of CA15-3 antibody were activated by incubation with a solution containing 0.4 M EDC and 0.1 M NHS for 0.5 h, and then incubated with the PEDOT/Pep/AuNP/GCE for 2 h at 37°C. After thorough rinsing, the stable Ab/PEDOT/Pep/AuNP/GCE biosensor was obtained. The biosensor was incubated with different concentrations of CA15-3, the change of current signals before and after specific binding was measured by DPV in the range of −0.2 to 0.6 V.

2.5. Cell adhesion test

For cell adhesion study, the Michigan Cancer Foundation-7 (MCF-7) cells were cultured in Dulbecco's modified Eagle's medium (DMEM) and stored in an incubator with a humidified 5.0% CO_2 at 37°C. Subsequently, the MCF-7 cells with a cell density of 1×10^5 cells mL^{-1} were incubated with AuNP, Pep/AuNP, and

PEDOT/Pep/AuNP modified substrate for 24 h at 37°C and gently rinsed with PBS to remove unattached cells. Then Fluorescein Diacetate (FDA) was used to stain the active MCF-7 cells absorbed on the surfaces by fluorescence microscopy using an excitation wavelength at 488 nm. Finally, images were captured to monitor MCF-7 adhesion on different surfaces.

2.6. Detection of CA15-3

DPV is a sensitive and powerful technique of quantitative detection. DPV measurements were carried out in PBS (10 mM, pH 7.4) containing 5.0 mM $[Fe(CN)_6]^{3-/4-}$ and 0.1 M KCl. The scan range was taken from –0.2 V to 0.6 V with incr. E 0.004 V, amplitude 0.05 V, pulse width 0.05 s, sampling width 0.0167 V and pulse period 0.2 s. After incubation with different concentration of the target CA15-3 and thorough washing with PBS, the current changes were recorded accordingly.

2.7. Preparation of clinical human serum sample

All serum samples of breast cancer patients were prepared by centrifugation of fresh blood at 10000 rpm for 5 min. The supernatants were collected. Then serum samples were stored at −80°C and thawed before use. Finally, they were diluted with PBS (10 mM, pH 7.4) and detected with the biosensor.

3 Results and discussions

3.1. Investigation of the newly designed peptides

It has been reported that peptide with a specific structure can be endowed with many unique functions on account of its diversity of amino acids and controllability of sequences (Kwon et al. 2019; Tao et al. 2017; Walsh and Knecht 2017). The isoelectric point (PI) is an important parameter to maintain the electrical neutrality of designed peptide. The relationship between the net charge and pH of the designed multifunctional peptide, and reference peptide, therefore, was calculated. The PI of the designed peptide with the sequence of CAEAEPPPPQEQKQEQK is 4.17 (Fig. S1A), and the measured zeta potential is −13.1 mV (Fig. S1A, B), indicating that the whole peptide chain is negatively charged due to the influence of the doping part. While the reference peptide (designed peptide without the doping part: PPPPQEQKQEQK), which is the peptide sequence exposed on the electrode surface after controlled doping of the designed peptide into the PEDOT, is electrically neutral (PI = 6.57, the zeta potential is near to 0 mV) (Fig. S1A, B), indicating that it has potential antifouling performance (avoid nonspecific adsorption through charge attraction).

The secondary conformation of polyproline-generated helix for the reference peptide was determined by circular dichroism (CD) spectrum (Fig. S1C), with a negative absorption band around 205 nm and a relatively weaker positive band near 225 nm. Such a secondary structure of the peptide sequence is preferred to achieve an orderly structure and a higher density of the antifouling peptide layer (Liu et al. 2018; Nowinski et al. 2012).

To evaluate the wettability of antifouling peptide modified surfaces, the static

water contact angles of bare GCE, AuNP/GCE and reference peptide modified surface (Reference Pep/AuNP/GCE) were presented in Fig. S1D. GCE surface showed a water contact angle of 54.8°. After modification with AuNPs, the original contact angle increased to 71.3°, indicating a more hydrophobic interface of electrodeposited AuNPs (Wang et al. 2018b). Further modification with reference peptide, however, significantly reduced the water contact angle to 28.5°, owing to the strong hydrophilicity of the zwitterionic peptide.

To further verify the antifouling performance of reference peptide, which is the peptide sequence exposed on the PEDOT surface, the nonspecific adsorption experiments on Au chips with and without the reference peptide were evaluated by surface plasmon resonance (SPR). Dynamic adsorption processes were recorded in Fig. S2, suggesting a very small change of ΔSPR and less protein-adsorption capacity (ca. 7.11 ng cm^{-2}) for the peptide-coated surface, in contrast to the bare Au surface with a strong adsorption of bovine serum albumin (BSA) (ca. 124.04 ng cm^{-2}) (Xia et al. 2019; Ye et al. 2016).

3.2. Characterization of the biosensing interfaces

The biosensor fabrication process was characterized using XPS and DPV. XPS data of different modified electrode surfaces were recorded in Fig. S3. As shown in Fig. S3A, the photoelectron signal of AuNPs on GCE emerged obviously two strong spectral bands as the characteristic peaks of Au $4f_{7/2}$ at 84 eV and Au $4f_{5/2}$ at 88 eV (As seen in the inset of Fig. S3A) (Wang et al. 2018b; Xu et al. 2017). When the

peptides were anchored on the AuNPs, the photoelectron peak of N 2s at 409 eV from peptide and the weaker signal of S 2p at 162 eV from the cysteine residues were observed (Fig. S3A) (Wang et al. 2017). After the electrodeposition of PEDOT on the surface, the photoelectron signal of S 2p increased remarkably, and the peak of Au 4f further declined (Fig. S3B). After the immobilization of Ab as a macromolecular protein, the peak value of N 2s significantly increased, and simultaneously, the peak of Au 4f decreased drastically (Fig. S3C). What's more, the detailed statistics of the content of elements on different modified electrode surfaces were shown in Table S1. These characteristics confirmed successful modification of the electrode step by step, and the successful construction of the biosensor.

DPV was carried out to monitor changes of current signal during the step-by-step modification process in 5.0 mM $[Fe(CN)_6]^{3-/4-}$ solution (10 mM PBS, pH 7.4) containing 0.1 M KCl. The oxidation peak of $[Fe(CN)_6]^{3-/4-}$ probe on AuNP/GCE (Fig. 1, curve b) was stronger than that on bare GCE (Fig. 1, curve a). The reason lies in that, on the one hand, the deposition of AuNPs increases the surface area of the electrode, on the other hand, AuNPs can promote the electron transfer of the probe on the electrode surface. After multifunctional peptide was self-assembled onto AuNP/GCE, the oxidation peak current of the probe decreased significantly, ascribed to the poor conductivity of the peptide (Fig. 1, curve c). However, the current signal was dramatically increased after the electrodeposition PEDOT on the electrode surface (Fig. 1, curve d), owing to excellent conductivity of PEDOT. After the immobilization of Ab, a declined current was obtained (Fig. 1, curve e), as the

non-conductive Ab will block the electron transfer of the probe. Once combined with antigens, the current signal of the biosensor further declined (Fig. 1, curve f) owing to the blocking effect of the antigens. CA12-5 was selected as a representative of the negative control. Excitingly, the experiment of the negative control showed that the current value of the biosensor dropped only slightly after incubating with CA12-5 (Fig. 1, curve g), which confirmed that the change of the current signal was indeed due to the specific binding of the antigen to the antibody on the electrode. Therefore, the results confirmed the successful construction of the CA15-3 biosensor.

3.3. Characterization of antifouling performance

To verify the antifouling capability of the peptide, anti-cell-adhesion performance of the substrates modified with AuNP, Pep/AuNP and PEDOT/Pep/AuNP, respectively, was evaluated using a confocal laser microscope (Fig. 2). As shown in Fig. 2A, many MCF-7 cells were nonspecifically attached to the AuNPs modified surface. While on the Pep/AuNP modified surface, the number of attached cells decreased significantly (Fig. 2B), suggesting that peptide is effective in preventing the adhesion of cells. Interestingly, the anti-cell-adhesion performance was further improved after the electrodeposition of PEDOT (Fig. 2C), owing to the fact that the negatively charged doping sequence was totally doped into the PEDOT film, and the antifouling sequence of the peptide was stretched out of the PEDOT surface, which exhibited excellent antifouling performance.

The antifouling performance of electrode surfaces with and without peptide was

further studied in single protein solutions containing BSA (negatively charged), myoglobin (Mb, neutral in charge) and lysozyme (Lys, positively charged), respectively. As shown in Fig. S4, the current signal changes ($(-\Delta I/I_0)\%$, $\Delta I = I - I_0$, I_0 and I refer to the oxidation peak current value of 5.0 mM $[Fe(CN)_6]^{3-/4-}$ before and after incubation with different concentrations of a single protein.) of the AuNP/GCE surface before and after incubation in protein solutions for 30 min were significantly larger than those of the PEDOT/peptide surface. Similar results of antifouling performance of electrode surfaces can also be seen in different concentrations of human serum, as illustrated in Fig. 3. The rates of signal change of PEDOT/Pep/AuNP/GCE surface were only 2.27% and 5.75% after soaking in 10% and 25% (V/V) human serum, respectively. More importantly, even for the prepared biosensor with antibodies immobilized, the rates of signal change of the Ab/PEDOT/Pep/AuNP/GCE surface still remained very low. The corresponding original DPV curves are shown in Fig. S5. These results indicate excellent antifouling capability of the PEDOT surface planted with designed antifouling peptides, even after further immobilization of certain recognizing biomolecules as biosensing probes.

Long term antifouling performance is also an important factor for sensors, especially implanted sensing devices. An evaluation of prolonged-periods antifouling performance for the PEDOT/Pep/AuNP/GCE in complex biological media is shown in Fig. 4. During the continuous testing lasted for 10 days, the current signal only decreased by 5.00% compared with the initial value (lasting for 30 days, the electrochemical signal only decreased by 12.36%). While under the same conditions,

the signal of the surface without antifouling peptides and PEDOT (AuNP/GCE) decreased very quickly, and continually collapsed by 94.54% in 30 days (Fig. 4). The results indicate that the design strategy of peptide combining doping and antifouling functions is successful, and the PEDOT surface planted with peptides possesses excellent long-term and stable antifouling performance, which is ideal for the development of implantable sensing devices.

3.4. Optimization of deposition time of PEDOT

Deposition time of PEDOT here is important to control the thickness of the formed PEDOT film, as well as the performance of the biosensor, including the antifouling and sensing performances. Antifouling capabilities of electrode surfaces electrodeposited with different thickness of PEDOT were investigated, as shown in Fig. 5A. When the deposition time was shorter than 8 s, the current signal change (represents the fouling effect) was significant, because part of the negatively charged doping sequence is exposed on the PEDOT surface, and it will adsorb positively charged proteins. When the deposition time was longer than 8 s, part of the antifouling peptide will be embedded in the formed PEDOT film, leading to reduced antifouling performance of the surface. The minimum of fouling effect was obtained at 8 s, the time that the doping sequence was exactly doped into the PEDOT. Similarly, 8 s was also the optimum deposition time for the sensing signal of the biosensor, as shown in Fig. 5B. Therefore, optimized time for the electrodeposition of PEDOT was 8 s.

3.5. Electrochemical detection of CA15-3

In order to achieve the best performance for the biosensor, the incubation time for antigens to associate with the immobilized antibodies was investigated (Fig. S6). The current signal increased with the incubation time of CA15-3 and achieved a maximum value at 2.5 h, and then remained almost stable with further increase of the incubation time, indicating the binding equilibrium at the incubation time of 2.5 h. Under optimized experimental conditions, the electrochemical biosensor response to a series of CA15-3 concentrations ranging from 0.001 to 1000 U mL^{-1} is shown in Fig. 6A. Linear fitting function of the biosensor is $-\Delta I$ (μA) = 3.203 log C + 10.15 with correlation coefficient (R^2) of 0.9986 (Fig. 6B), and the limit of detection (LOD) for this biosensor is calculated to be 0.32 mU mL^{-1} (S/N = 3). While in the biosensor without PEDOT deposition (Ab/Pep/AuNP/GCE), the linear range is 0.1-1000 U mL^{-1}, with the LOD of 35.64 mU mL^{-1} (Fig. S7A), and the biosensor fabricated through co-electrodeposition of multifunctional peptide and PEDOT (Ab/PEDOT-Pep/AuNP/GCE), the linear range is 0.01-1000 U mL^{-1}, with the LOD of 3.34 mU mL^{-1} (Fig. S7B). The sensitivity of the biosensor is also better than that of previously reported CA15-3 sensors (Park et al. 2014) and electrochemiluminescence method (Hamd-Ghadareh et al. 2018; Jiang et al. 2015). The prepared biosensor (Ab/PEDOT/Pep/AuNP/GCE) showed a wider detection range and lower LOD, which may be ascribed to the excellent conductivity, stability and biocompatibility of the substrate composed of doping peptide and PEDOT, and the outstanding antifouling

property of the tightly packed antifouling peptide surface, which provided extremely low noisy signal for higher specific recognition of CA15-3.

3.6. Selectivity and reproducibility of the CA15-3 biosensor

The selectivity of the antifouling biosensor was evaluated based on DPV responses to several proteins possibly co-existed with the target protein in the serum, including CA12-5, CEA, AFP, PSA, and HSA. As can be seen from Fig. S8, the biosensor showed excellent selectivity toward its target CA15-3, and it exhibited negligible responses towards nonspecific proteins even at much higher concentrations.

In addition, the intra-batch and inter-batch reproducibilities of the antifouling biosensor were also evaluated. For the detection of 100 U mL^{-1} CA15-3, the relative standard deviation (RSD) of the intra- (Fig. S9A, C) and inter-assay (Fig. S9B, D) are 0.24% and 1.64%, respectively (n = 7). The results proved excellent stability and reproducibility of the biosensor based on PEDOT and multifunctional peptide.

3.7. Clinical serum sample analysis

To evaluate the potential clinical application of the biosensor, clinical samples from five patients with breast cancer were tested. All human serum samples were diluted to 10% by volume (V/V). As shown in Fig. 7, the analysis results obtained by the biosensor were highly consistent with those from the data of detection by clinical method (Chemiluminescence immunoassay) via linear fitting, with the R^2 of 0.9955, which indicated that the newly designed antifouling CA15-3 biosensor was reliable

for the detection in practical serum samples.

4. Conclusion

A new strategy for the construction of conducting polymer surfaces with excellent antifouling capability was developed based on designed multifunctional peptides. Through finely controlled electrodeposition of PEDOT, the doping sequence of the designed peptide can be exactly doped into the formed PEDOT, leaving the antifouling sequence of the peptide stretched out of the PEDOT film. The obtained PEDOT film planted with antifouling peptide exhibited excellent antifouling capability, and compared with traditional antifouling strategies, this strategy of assembling multifunctional peptides first and then depositing PEDOT can obtain outstanding antifouling performance with a well-packed antifouling layer and excellent electrical conductivity as well as long-term antifouling ability. Once immobilized with recognizing probes, low fouling electrochemical biosensors capable of assaying targets in complex biological media were easily developed. Given the versatility of bio-recognize elements (aptamer, antibody, and etc.), this antifouling platform can be readily used for sensitive detection of many kinds of analytes through immobilizing with bio-recognition elements. Therefore, the proposed antifouling strategy based on PEDOT planted with antifouling peptides has a bright prospect not only in the direct detection of targets in complex media but also as an antifouling versatile platform in the field of biosensing.

Appendix A. Supporting information

Supplementary data associated with this article can be found in the online version at doi: 10.1039/x0xx00000x

Acknowledgment

We acknowledge financial support from the Shandong Provincial Natural Science Foundation (ZR2019MB039, ZR2017BEM014), the National Natural Science Foundation of China (21675093, 21974075, 51702228), the Taishan Scholar Program of Shandong Province of China (ts20110829), the Shandong Key Laboratory of Biochemical Analysis (SKLBA1905) and the Doctoral Found of Taishan University (Y-01-2018018, 2019HX099).

References

Cao, B., Lee, C., Zeng, Z., Cheng, F., Xu, F., Cong, H., Cheng, G., 2016. Chem. Sci. 7(3), 1976-1981.

Cui, M., Song, Z., Wu, Y., Guo, B., Fan, X., Luo, X., 2016. Biosens. Bioelectron. 79, 736-741.

Ge, S., Zhang, L., Zhang, Y., Lan, F., Yan, M., Yu, J., 2017. Nanoscale. 9(13), 4366-4382.

Hamd-Ghadareh, S., Salimi, A., Parsa, S., Fathi, F., 2018. Int. J. Biol. Macromol. 118, 617-628.

Hui, N., Sun, X., Niu, S., Luo, X., 2017. ACS Appl. Mater. Interfaces. 9, 2914-2923.

Jiang, X., Wang, H., Yuan, R., Chai, Y., 2015. Biosens. Bioelectron. 63(20), 33-38.

Kwon, O.S., Song, H., Park, T.H., Jang, J., 2019. Chem. Rev. 119(1), 36-93.

Liu, B., Li, Q., Zhang, B., Cui, Y., Chen, H., Chen, G., Tang, D., 2011. Nanoscale 3(5), 2220-2226.

Liu, N., Xu, Z., Morrin, A., Luo, X., 2019a. Anal. Methods. 11(6), 702-711.

Liu, N., Hui, N., Davis, J.J., Luo, X., 2018. ACS Sen. 3(6), 1210-1216.

Liu, N., Song, J., Lu, Y., Davis, J.J., Gao, F., Luo, X., 2019b. Anal. Chem. 91(13), 8334-8340.

Liu, X., Xiao, T., Wu, F., Shen, M., Zhang, M., Yu, H., Mao, L., 2017. Angew. Chem., Int. Ed. 56(39), 11802-11806.

Ma, L., Jayachandran, S., Li, Z., Song, Z., Wang, W., Luo, X., 2019. J. Electroanal. Chem. 840, 272-278.

Martín, M., Salazar, P., Jiménez, C., Lecuona, M., Ramos, M.J., Ode, J., Alcoba, J., Roche, R., Villalonga, R., Campuzano, S., Pingarrón, J.M., González-Mora, J.L., 2015. Anal. Chim. Acta 887, 51-58.

Nowinski, A.K., Sun, F., White, A.D., Keefe, A.J., Jiang, S., 2012. J. Am. Chem. Soc. 134(13), 6000-6005.

Park, S., Singh, A., Kim, S., Yang, H., 2014. Anal. Chem. 86(3), 1560-1566.

Tao, K., Makam, P., Aizen, R., Gazit, E., 2017. Science. 358(6365).

Vaisocherová, H., Brynda, E., Homola, J., 2015. Anal. Bioanal. Chem. 407(14), 3927-3953.

Walsh, T., Knecht, M.R., 2017. Chem. Rev. 117(20), 12641-12704.

Wang, G., Morrin, A., Li, M., Liu, N., Luo, X., 2018a. J. Mat. Chem. B 6(25), 4173-4190.

Wang, G., Han, R., Su, X., Li, Y., Xu, G., Luo, X., 2017. Biosens. Bioelectron. 92, 396-401.

Wang, G., Su, X., Xu, Q., Xu, G., Lin, J., Luo, X., 2018b. Biosens. Bioelectron. 101, 129-134.

Wang, W., Cui, M., Song, Z., Luo, X., 2016. Rsc Adv. 6(91), 88411-88416.

Wu, H., Lee, C., Wang, H., Hu, Y., Young, M., Han, Y., Xu, F., Cong, H.B., Cheng, G., 2018. Chem. Sci. 9(9), 2540-2546.

Wu, J., Chen, J., Liu, K., Luo, S., 2019. ACS Appl. Mater. Interfaces 11(24), 21294-21307.

Wu, L., Qu, X., 2015. Chem. Soc. Rev. 44(10), 2963-2997.

Xia, Y., Adibnia, V., Huang, R., Murschel, F., Faivre, J., Xie, G., Olszewski, M., De Crescenzo, G., Qi, W., He, Z., Su, R., Matyjaszewski, K., Banquy, X., 2019. Angew. Chem. 131(5), 1322-1328.

Xu, S., Wu, Y., Sun, X., Wang, Z., Luo, X., 2017. J. Mat. Chem. B 5(22), 4207-4213.

Ye, H., Xia, Y., Liu, Z., Huang, R., Su, R., Qi, W., Wang, L., He, Z., 2016. J. Mat. Chem. B 4(23), 4084-4091.

Captions

Scheme 1. Schematic fabrication process of the electrochemical CA15-3 biosensor based on antifouling peptide planted in PEDOT film.

Figure 1. Electrochemical responses of different modified electrodes: (a) bare GCE, (b) AuNP/GCE, (c) Pep/AuNP/GCE, (d) PEDOT/Pep/AuNP/GCE, (e) Ab/PEDOT/Pep/AuNP/GCE, (f) CA15-3/Ab/PEDOT/Pep/AuNP/GCE, and (g) CA12-5/Ab/PEDOT/Pep/AuNP/GCE. Curve g (almost overlapped with curve e), represents the response of the biosensor after incubation in the negative control of 100 ng mL^{-1} CA12-5 solution (10 mM PBS, pH 7.4).

Figure 2. Anti-cell-adhesion performance of (A) AuNP, (B) Pep/AuNP, and (C) PEDOT/Pep/AuNP modified substrate incubated with MCF-7 cells for 24 h at 37°C.

Figure 3. The current signal rate of change of the surface without peptide (AuNP/GCE), with peptide (PEDOT/Pep/AuNP/GCE) and CA15-3 biosensor (Ab/PEDOT/Pep/AuNP/GCE) in a series of healthy human serums. $\Delta I = I - I_0$, I_0 and I refer to the oxidation peak current value of 5.0 mM $[Fe(CN)_6]^{3-/4-}$ before and after incubation with different concentrations of serum. Error bars represent the standard deviations of three repeated determinations.

Figure 4. Long-term antifouling performance of PEDOT/Pep/AuNP/GCE (A) and AuNP/GCE (B) surfaces in 10% (V/V) human serum samples for an extended period (30 min to 30 days). Error bars represent the standard deviations of three repeated determinations.

Figure 5. The effect of PEDOT deposition time on antifouling performance (A) and

sensing response (B) of the biosensor (Ab/PEDOT/Pep/AuNP/GCE). The schematic diagrams of inset in (A) corresponding to the PEDOT deposition time is 5 s, 8 s and 20 s respectively from left to right. The concentration of CA15-3 is 1000 U mL^{-1}. Error bars represent the standard deviations of three repeated determinations.

Figure 6. (A) DPV response of the biosensor incubated with different CA15-3 concentrations, curves from a to h represent 0, 0.001, 0.01, 0.1, 1, 10, 100, 1000 U mL^{-1} CA15-3, respectively. Inset: DPV curves after background subtraction, $\Delta I = I - I_0$, I_0 and I refer to the oxidation peak current value of 5.0 mM $[Fe(CN)_6]^{3-/4-}$ before and after incubation with different CA15-3 concentrations in PBS (10 mM, pH 7.4). (B) Current change of the biosensor upon a function of CA15-3 concentrations. The inset shows the corresponding calibration curve. Error bars represent the standard deviations of three repeated determinations.

Figure 7. Real sample analysis of CA15-3 in 10% (V/V) serum of breast cancer patients: CA15-3 concentrations in five different serum samples determined by the CA15-3 biosensor vs detection by chemiluminescence immunoassay (clinical diagnosis method). Error bars represent the standard deviations of three repeated determinations.

Figures

Scheme 1.

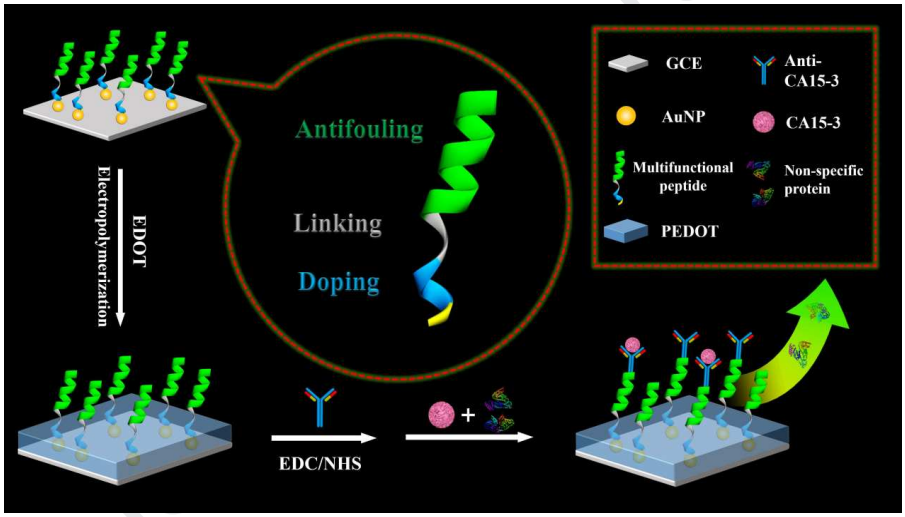

Figure 1.

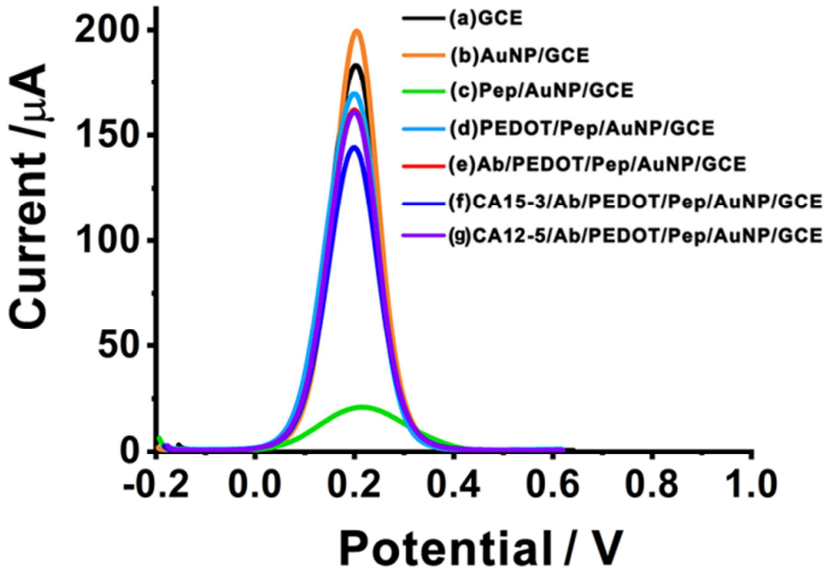

Figure 2.

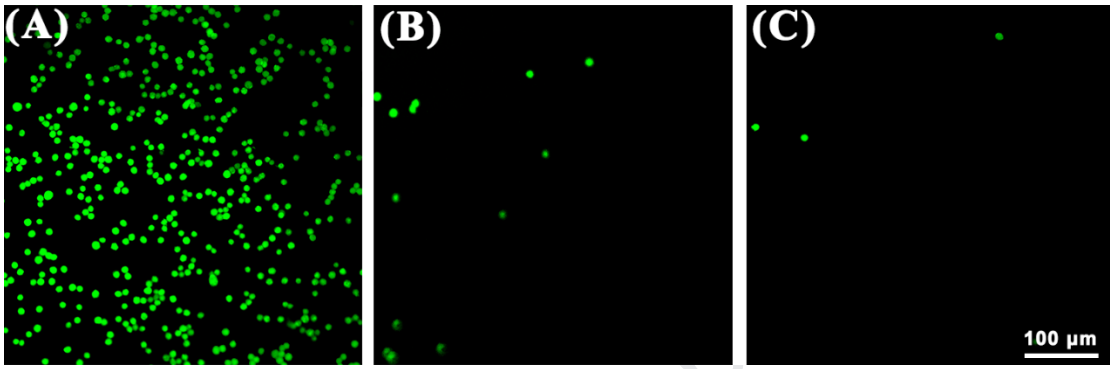

Figure 3.

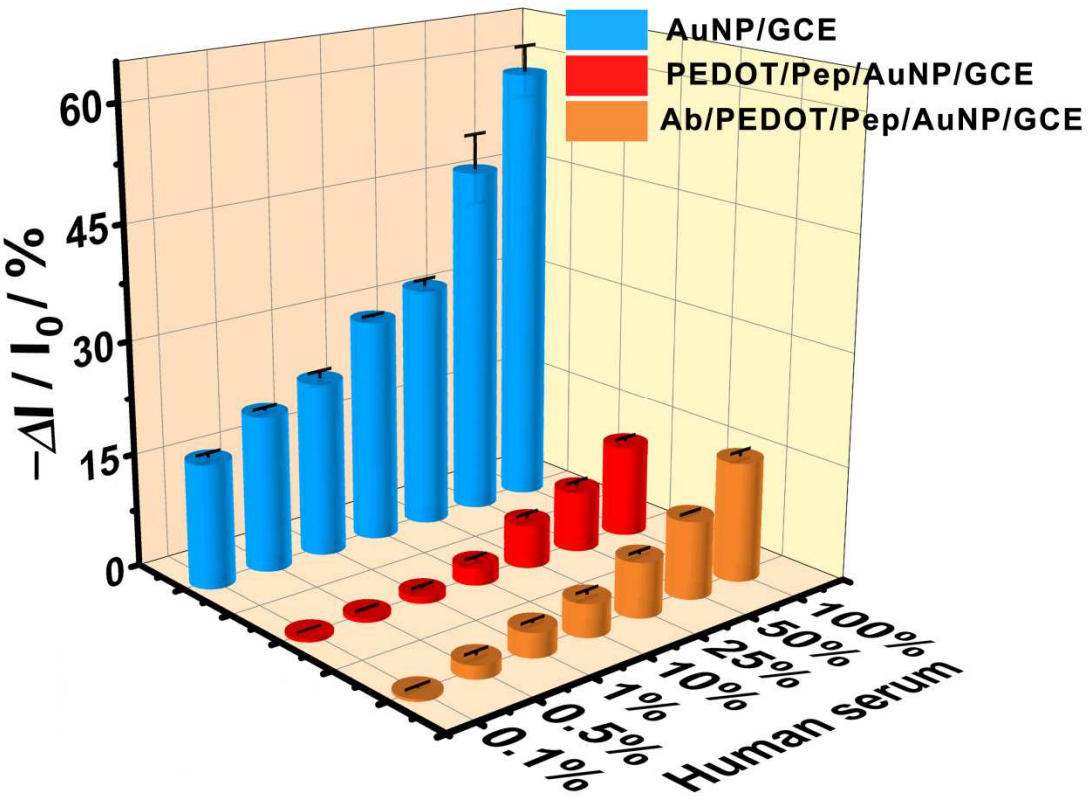
AuNP/GCE
PEDOT/Pep/AuNP/GCE
Ab/PEDOT/Pep/AuNP/GCE
−ΔI / I0 / %
0
15
30
45
60
0.1%
0.5%
1%
10%
25%
50%
100%
Human serum

Figure 4.

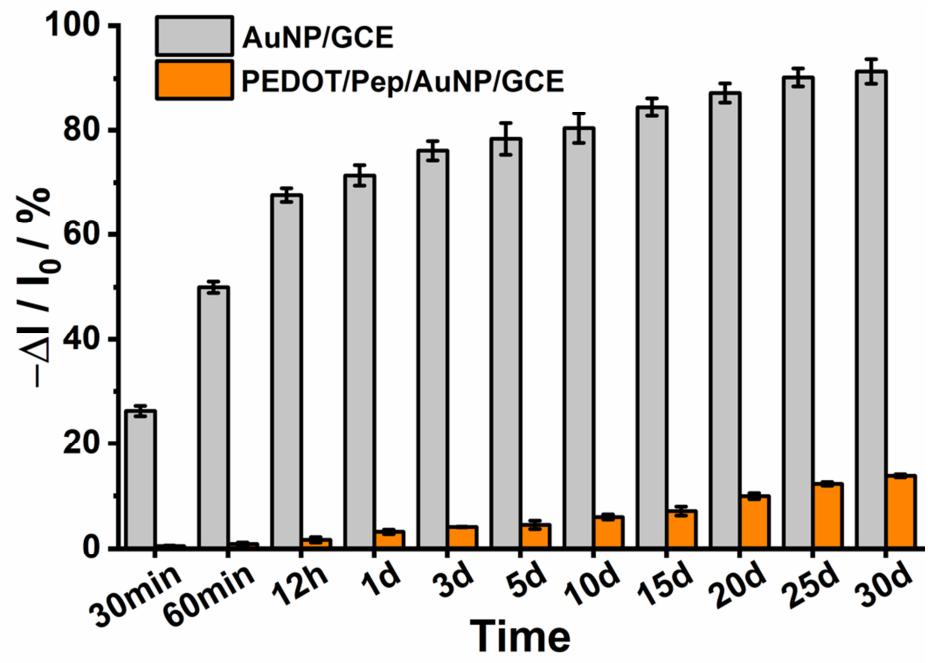

Figure 5.

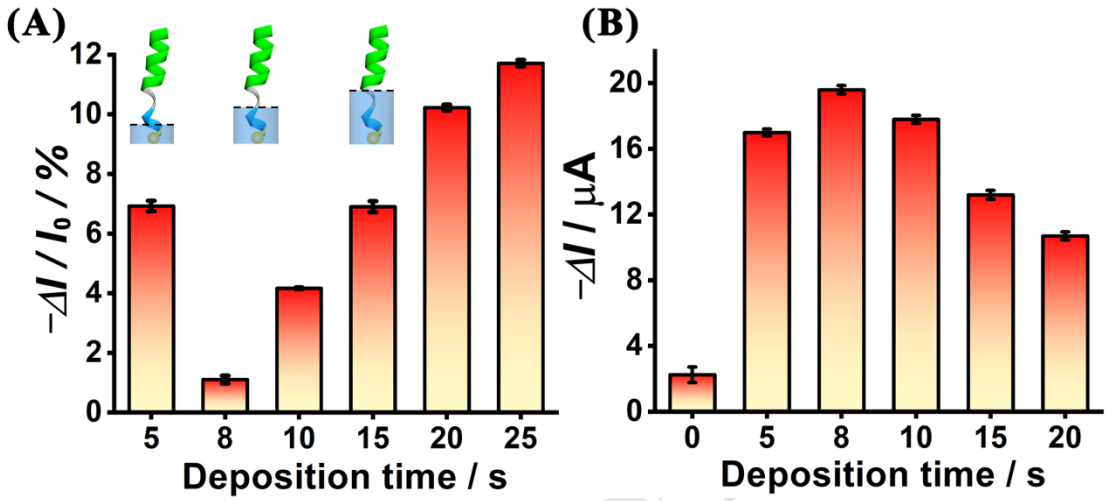

Figure 6.

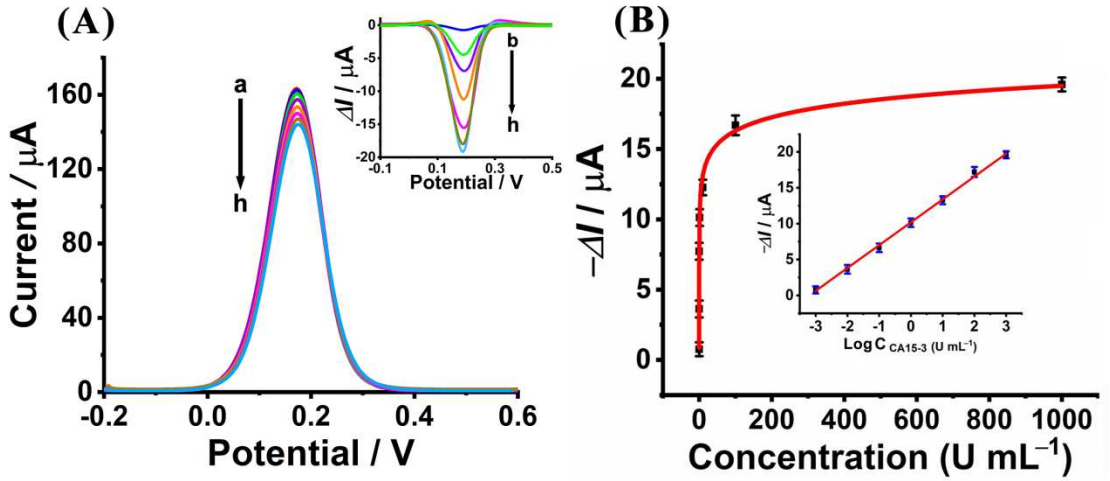

Figure 7.

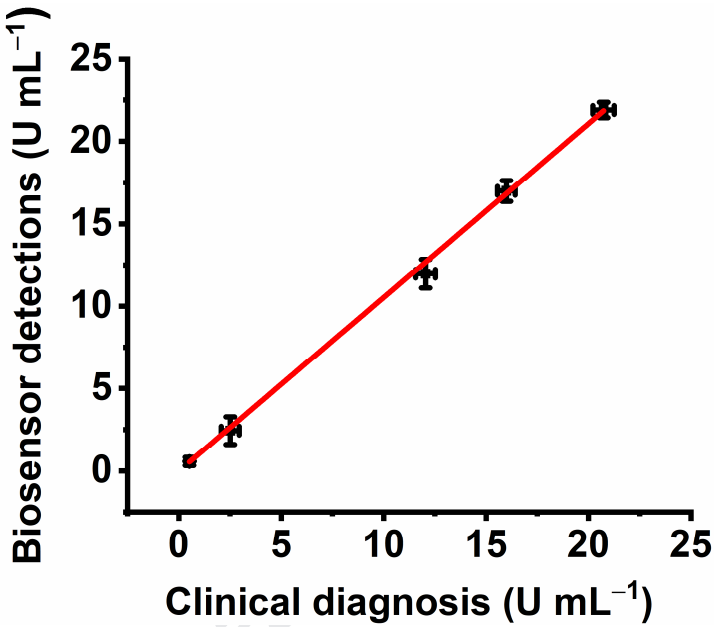

Highlights

- An effective antifouling substrate for the construction of biosensors was prepared;
- PEDOT planted with antifouling peptide was synthesized through electrochemical polymerization;
- The antifouling biosensor supported the detection of CA15-3 in serum samples.

Declaration of interests

☒ The authors declare that they have no known competing financial interests or personal relationships that could have appeared to influence the work reported in this paper.

☐The authors declare the following financial interests/personal relationships which may be considered as potential competing interests: